Control of Floret Symmetry by *RAY3*, *SvDIV1B*, and *SvRAD* in the Capitulum of *Senecio vulgaris*[1][OPEN]

Helena Maria Pereira Garcês, Victoria M. R. Spencer, and Minsung Kim*

Faculty of Life Sciences, University of Manchester, Oxford Road, Manchester M13 9PT, United Kingdom

ORCID IDs: 0000-0002-3703-7531 (H.M.P.G.); 0000-0002-9930-1377 (V.M.R.S.); 0000-0002-8470-793X (M.K.).

All members of Asteraceae, the largest flowering family, have a unique compressed inflorescence known as a capitulum, which resembles a solitary flower. The capitulum often consists of bilateral (zygomorphic) ray florets and radial (actinomorphic) disc florets. In *Antirrhinum majus*, floral zygomorphy is established by the interplay between dorsal petal identity genes, *CYCLOIDEA* (*CYC*) and *RADIALIS* (*RAD*), and a ventral gene *DIVARICATA* (*DIV*). To investigate the role of *CYC*, *RAD*, and *DIV* in the development of ray and disc florets within a capitulum, we isolated homologs of these genes from an Asteraceae species, *Senecio vulgaris* (common groundsel). After initial uniform expression of *RAY3* (*CYC*), *SvRAD*, and *SvDIV1B* in ray florets only, *RAY3* and *SvRAD* were exclusively expressed in the ventral petals of the ray florets. Our functional analysis further showed that *RAY3* promotes and *SvDIV1B* represses petal growth, confirming their roles in floral zygomorphy. Our results highlight that while floral symmetry genes such as *RAY3* and *SvDIV1B* appear to have a conserved role in petal growth in both *Senecio* and *Antirrhinum*, the regulatory relationships and expression domains are divergent, allowing ventral petal elongation in *Senecio* versus dorsal petal elongation in *Antirrhinum*. In *S. vulgaris*, diversification of *CYC* genes has led to novel interactions; *SvDIV1B* inhibits *RAY3* and *SvRAD*, and may activate *RAY2*. This highlights how recruitment of floral symmetry regulators into dynamic networks was crucial for creating a complex and elaborate structure such as the capitulum.

Floral symmetry plays an essential role in pollination efficiency and, thus, in flower evolution. Based on floral symmetry, flowers can be classified as zygomorphic or actinomorphic. Zygomorphic flowers have a single plane of symmetry (bilateral), whereas actinomorphic flowers have multiple planes of symmetry (radial; Endress, 1999). Floral zygomorphy has independently evolved multiple times within the angiosperm lineage (Citerne et al., 2010). It has been proposed that zygomorphic flowers first arose from actinomorphic flowers around 70 million years ago, which coincided with the species radiation of pollinators. This suggests that flower-pollinator interactions may be a major driver in the evolution of floral zygomorphy (Crepet, 1996).

In *Antirrhinum majus* (Lamiales), the key genetic regulators of floral zygomorphy have been identified. The *TCP* transcription factors *CYCLOIDEA* (*CYC*) and *DICHOTOMA* (*DICH*) have partially redundant functions and determine the dorsal region of the flower by differentially regulating the rate of cell growth in the developing floral organs (Luo et al., 1999, 1996; Zhang et al., 2010; Preston and Hileman, 2009). These genes belong to the *CYC2* clade (Howarth and Donoghue, 2006) and are expressed in the dorsal petals of flowers (Almeida et al., 1997; Luo et al., 1999, 1996). The MYB-domain transcription factors *RADIALIS* (*RAD*; Corley et al., 2005) and *DIVARICATA* (Almeida and Galego, 2005; Almeida et al., 1997) also participate in regulating floral symmetry. *RAD* is expressed dorsally and is positively regulated by *CYC* (Costa et al., 2005), and *rad* mutants, in similarity to *cyc* mutants, form partially ventralized flowers (Luo et al., 1996). The *DIV* gene promotes ventral petal identity and loss of *DIV* function leads to lateralized ventral petals (Almeida et al., 1997). *RAD* acts antagonistically to *DIV* (Corley et al., 2005), repressing its activity in the dorsal petals and causing *DIV* activity to be restricted to the ventral and lateral petals (Hileman, 2014; Raimundo et al., 2013).

In the evolution of floral zygomorphy, *CYC* activity has been independently recruited in many species. While *CYC* orthologs maintained a conserved role in controlling petal growth, changes in their expression domains were crucial for the shift between zygomorphic and actinomorphic flowers (Busch and Zachgo, 2007; Kim et al., 2008; Zhang et al., 2010; Howarth et al., 2011; Hileman, 2014; Feng et al., 2006; Wang et al., 2008; Zhong and Kellogg, 2015a, 2015b). For example, a gain of dorsal-specific *CYC* expression caused floral zygomorphy in the Malpighiaceae family (Zhang et al., 2010), whereas a uniform *CYC* expression in all petals

[1] This work was supported by the Biotechnology and Biological Sciences Research Council Research Grant BB/I012982/1.

* Address correspondence to minsung.kim@manchester.ac.uk.

The author responsible for distribution of materials integral to the findings presented in this article in accordance with the policy described in the Instructions for Authors (www.plantphysiol.org) is: Minsung Kim (minsung.kim@manchester.ac.uk).

M.K. conceived the project and the original research plans and supervised the project; H.M.P.G. conceived research plan, designed the experiments, performed most of the experiments, and analyzed the data; V.M.R.S. generated the constructs; H.M.P.G. drafted the article and all authors revised the article.

[OPEN] Articles can be viewed without a subscription.

www.plantphysiol.org/cgi/doi/10.1104/pp.16.00395

resulted in a regain of floral actinomorphy in a legume species (Citerne et al., 2006). While the importance of *CYC* genes in the evolution of floral zygomorphy has been studied extensively in many species, evidence of *RAD* and *DIV* involvement is very limited. Recently, it has been proposed that the reversion to actinomorphic flowers in *Plantago lanceolata* is due to a loss of *RAD* from the genome (Reardon et al., 2014). In *Bournea leiophylla* (Gesneriaceae), loss of dorsal expression of *BlCYC* and *BlRAD* during the later stages of flower development led to up-regulation of *BlDIV* in the entire flower, which in turn generated a final actinomorphic structure (Zhou et al., 2008). In Lamiales, the *RAD* expression domain plays an important role in flower zygomorphy: The basal actinomorphic flowers in Lamiales had uniform *RAD* expression, whereas zygomorphic flowers in the clade showed dorsal/lateral *RAD* expression (Zhong and Kellogg, 2015b). In Dipsacales, *RAD* genes are duplicated (*RAD1*, *RAD2*, and *RAD3* groups) and only a subset of *RAD* genes appears to be expressed in the dorsal regions (Boyden et al., 2012). Furthermore, it has been shown that in the Dipsacales species, *Heptacodium miconioides*, *DIV-like* genes have also been duplicated and are differentially expressed among petals within a flower, suggesting *HmDIV* genes are vital for floral zygomorphy in this species (Howarth and Donoghue, 2009). Although these studies imply that *RAD* and *DIV* are involved in zygomorphy evolution, their suggested roles require further validation by functional analyses.

In the sunflower family (Asteraceae), the evolution of floral zygomorphy is more complex. Asteraceae species are characterized by having a capitulum, which is a compressed inflorescence consisting of two types of flowers: ray and disc florets. In the capitulum, disc florets are positioned in the center, surrounded by ray florets at the margin (Fig. 1, A–D). A disc floret has five evenly sized petals with radial symmetry (actinomorphic; Fig. 1G), while a ray floret has bilateral symmetry (zygomorphic; Fig. 1F) with three fused and elongated ventral petals and two reduced dorsal petals (Trow, 1912). In addition to controlling zygomorphy in solitary flowers such as *Antirrhinum*, the floral symmetry regulator *CYC* has acquired a novel role in determining floret identity (disc versus ray) within the capitulum (Kim et al., 2008; Broholm et al., 2008; Chapman et al., 2008). Much of this work has focused on the three model Asteraceae species: *Senecio vulgaris* (common groundsel), *Helianthus annuus* (sunflower), and *Gerbera hybrida* (gerbera; Kim et al., 2008; Broholm et al., 2008; Chapman et al., 2008).

Of the three *CYC* clades of the *CYCLOIDEA/TEOSINTE BRANCHED1-LIKE* (*CYC/TB1*) subfamily, the *CYC2* clade has highly diversified and duplicated within the Asteraceae lineage; six *CYC2* clade genes have been identified in both *G. hybrida* and *S. vulgaris*, and five in *H. annuus* (Tähtiharju et al., 2012; Broholm et al., 2008; Kim et al., 2008). Of these *CYC2* clade genes, some members are expressed exclusively in ray florets and also cause altered ray floret morphology when disrupted. For example, in *H. annuus*, *HaCYC2c* and *HaCYC2d* showed ray floret-specific expression (Chapman et al., 2008; Tähtiharju et al., 2012). Furthermore, overexpression of *HaCYC2c* due to an insertion in the promoter generated capitula with only ray florets, providing functional evidence for its role in ray formation (Chapman et al., 2012). In addition to ray and disc florets, the *G. hybrida* capitulum has zygomorphic trans florets that have intermediate features of both ray and disc florets. Among the *G. hybrida CYC2* clade members, *GhCYC2*, *GhCYC3*, *GhCYC4*, *GhCYC5*, and *GhCYC9* also showed ray/trans floret-specific expression (Broholm et al., 2008; Juntheikki-Palovaara et al., 2014) and overexpression of *GhCYC2* generated disc florets with ray floret features (Broholm et al., 2008; Preston and Hileman, 2009; Juntheikki-Palovaara et al., 2014). In agreement with the other species, two *CYC2* genes in *S. vulgaris*, *RAY1* and *RAY2*, were expressed only in the ray florets and were also shown to control ray versus disc floret identity (Kim et al., 2008).

In addition to determining floret identity, *CYC* control of ray floral zygomorphy also appears to be conserved in some cases. Functional analyses in *S. vulgaris* revealed that overexpression of *RAY1* reduced ventral petal growth in ray florets, while overexpression of *RAY2* promoted dorsal ray petal outgrowth to produce tubular ray florets (Kim et al., 2008). Further work in gerbera suggests that localized expression of *GhCYC2* to the ventral petals explains this zygomorphic phenotype (Broholm et al., 2008; Juntheikki-Palovaara et al., 2014); however, differential expression of *CYC2* clade genes in ventral and dorsal petals in other Asteraceae species has not yet been seen.

In order to better understand how floral symmetry is established in two distinct ray and disc florets within a capitulum in the Asteraceae family, we have investigated the role of a *CYC2* clade gene (*RAY3*) as well as two floral symmetry MYB domain regulators (*SvRAD* and *SvDIV1B*) in *S. vulgaris*. Our study revealed that during the early capitulum development, *RAY3*, *SvRAD*, and *SvDIV1B* showed uniform ray floret specific expression, suggesting that the *CYC-RAD-DIV* gene network was recruited into *S. vulgaris* capitula for zygomorphic ray floret formation. During ray floret petal development, *RAY3* and *SvRAD* expression was confined to emerging ray ventral petals, suggesting that ventral petal specific expression could play a role in establishing ray floret bilateral symmetry. Our functional analysis further showed that *RAY3* promotes and *SvDIV1B* represses petal growth. At the later capitula stages, prolonged *RAY3* and decreasing *SvDIV1B* expression may be crucial for the rapid ventral petal growth in the ray florets. Furthermore, during capitulum development, *RAY3* promotes *RAY1* and *RAY2*, while *SvDIV1B* inhibits *RAY3* and *SvRAD*, and activates *RAY2*. As well as reaffirming the recruitment of *CYC2* genes for ray identity in the Asteraceae lineage, our results highlight that floral symmetry genes such as *RAD* and *DIV* appear to have a conserved role in petal growth in both *Antirrhinum* and *Senecio*; however, their

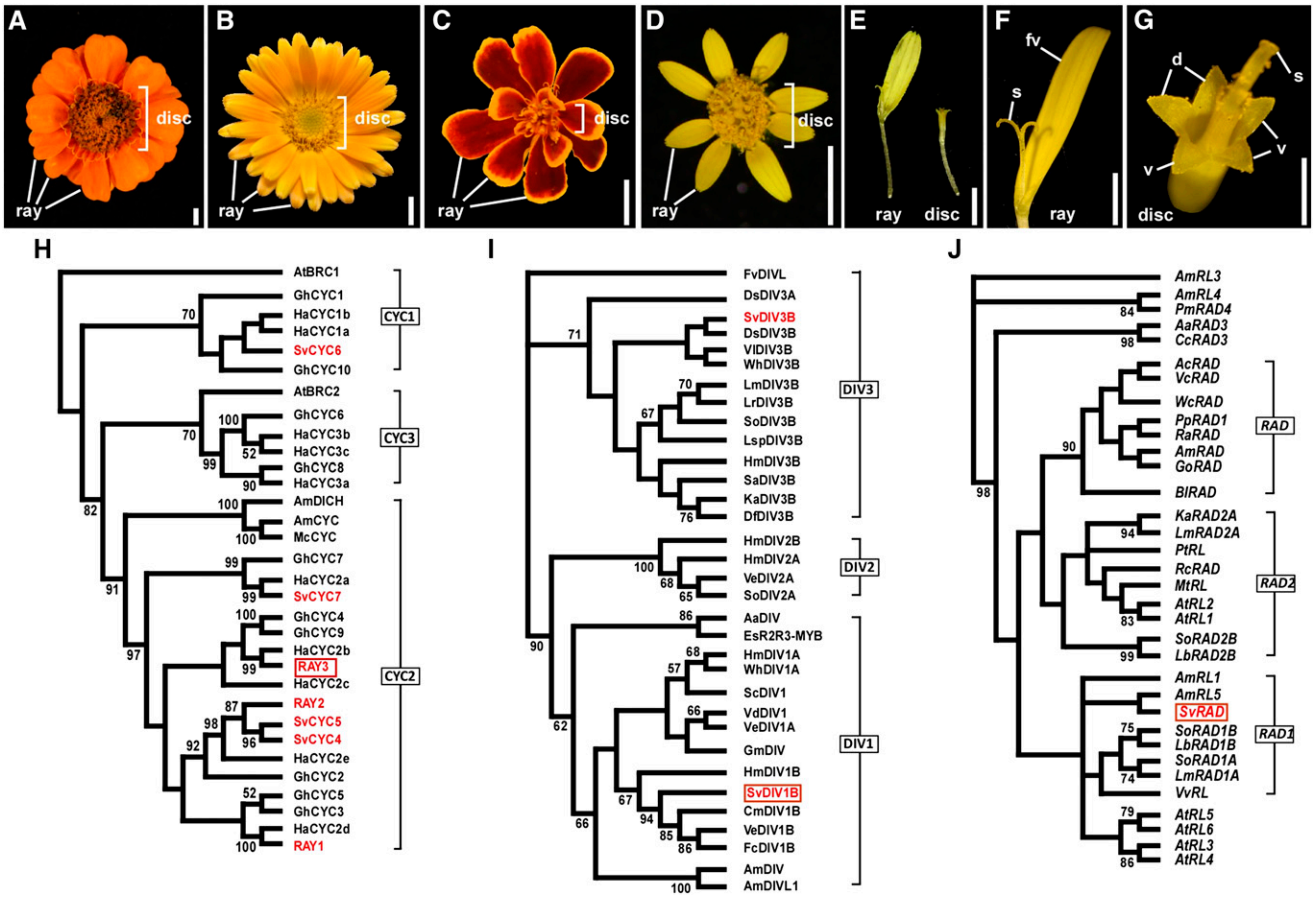

Figure 1. Capitulum and floret morphology in Asteraceae. A to D, Capitulum of *Zinnia elegans* (A), *Calendula officinalis* (B), *Tagetes patula* (C), and *S. vulgaris* (D). E to G, zygomorphic ray (E and F) and actinomorphic disc (E and G) floret of *S. vulgaris*. d, Dorsal petal; fv, fused three ventral petals; S, stigma; V, ventral petal. Bars = 5 mm (A–D), 2 mm (E), 1 mm (F), and 0.5 mm (G). H to J, ML phylogenetic tree analyses showing floral symmetry gene relationships among several species. ML trees were generated based on 99 amino acids including the conserved TCP and R domains for CYC, 95 amino acids that included the conserved SANT domain for DIV, and 83-bp DNA sequences including the conserved SANT domain for *RAD*. *S. vulgaris* (Sv) genes are colored in red. H, RAY3 clusters together with HaCYC2b (red rectangle). I, The ML three major clades are labeled as DIV1, DIV2, and DIV3. SvDIV1B protein falls into the DIV1 clade (red rectangle). J, *SvRAD* grouped with *AmRL5* (red rectangle). See "Materials and Methods" for the species abbreviations. Bootstrap values (500 replicates) greater than 50% are shown.

expression domains and regulatory relationships may differ to account for the varying flower symmetries in these two distant species. It appears that the *CYC-RAD-DIV* gene network has been reinvented in Asteraceae to recapitulate a functional flower by the arrangement of florets.

RESULTS

Gene Isolation and Phylogenetic Relationships

To determine the mechanism that controls floral symmetry within the capitulum, we have isolated a *CYC* homolog gene fragment (297 bp) from *S. vulgaris*. To be consistent with previously reported RAY1 and RAY2 CYC-like proteins in *S. vulgaris* (Kim et al., 2008), we have named our sequence *RAY3*. BLAST analysis showed that its protein sequence shared 100% similarity with *Senecio squalidus* CYC-like (accession no. JF299257) and 60% with *H. annuus* CYC2b proteins. The maximum likelihood (ML) phylogenetic relationship analysis based on partial TCP and R domain protein sequences (Broholm et al., 2008; Cubas et al., 1999) placed RAY3 in the CYC2 subclade as a HaCYC2b homolog (Fig. 1H; RAY3 in red rectangle), unlike other *Senecio* CYC2 proteins (SvCYC4, SvCYC5, and svCYC7).

Two *DIV* genes were also isolated from *S. vulgaris*. ML phylogenetic analysis based on MYB protein sequences (which included the conserved SANT domain and the DIV-like typical conserved Trp residues; Cubas et al., 1999; Corley et al., 2005) placed these two *DIV* genes distinctly in the clade of class *DIV1B* and *DIV3B* genes, respectively (Fig. 1I). We have therefore designated them as *SvDIV1B* and *SvDIV3B*. However, in this article, we focused on *SvDIV1B*

(Fig. 1I, red rectangle), which we found to be involved in capitulum development. The DIV1B protein sequence (274 amino acids) shared 67% identity with *A. majus* DIV.

Moreover, we have also isolated a 299-bp *RAD*-related gene fragment and showed that its protein (SvRAD) sequence was 72% identical to RAD from *Gratiola officinalis* (GoRAD). ML phylogenetic analysis revealed that our RAD-related protein was highly similar to RAD and RAD-LIKE proteins. Further ML phylogenetic analysis based on *RAD* and *RAD-like* DNA sequences that included the conserved SANT domain, placed *SvRAD* with *AmRAD-like5* in the *RAD1* clade (Fig. 1J, red rectangle).

Expression of *RAY3*, *SvDIV1B*, and *SvRAD* during *S. vulgaris* Capitulum Development

To reveal the roles of *RAY3*, *SvDIV1B*, and *SvRAD* during capitulum development, we investigated their expression patterns in stage 1 to 5 *S. vulgaris* capitula (for the details of stages, see "Materials and Methods") by RNA in situ hybridization. Results showed that all *RAY3*, *SvDIV1B*, and *SvRAD* mRNA transcripts accumulated in the emerging ray floret primordia of the stage 1 capitulum (Fig. 2, A, E, and I). Once disc and ray florets were formed (stage 3-4), high and uniform expression was detected for all three genes exclusively in ray florets but absent in disc florets (Fig. 2, B, C, F, G, and J). In stage 5 of capitulum development, *RAY3* and *SvRAD* were still highly expressed in ray florets but only in the ventral petals (Fig. 2, D and L). In contrast, *SvDIV1B* transcripts were not detectable in either dorsal or ventral petals of ray and disc florets (Fig. 2H), although very faint expression was detected in carpels (Fig. 2H, arrow).

In order to quantify *RAY3*, *SvDIV1B*, and *SvRAD* gene expression during later stages of *S. vulgaris* capitulum development, we performed quantitative RT-PCR (qRT-PCR) using ray florets, disc florets, and phyllaries from capitula at stages 6 to 8, as well as stems and leaves. The *RAY3* transcripts showed capitulum-specific expression (Fig. 3A). For all three stages, *RAY3* transcripts were significantly higher in ray florets, lower in disc florets and phyllaries, and almost absent from stems and leaves (Fig. 3A). *RAY3* is therefore constantly expressed in ray florets in all the developmental stages analyzed. Conversely, similar levels of *SvDIV1B* expression were initially detected for both ray and disc florets (Fig. 3B) as lateral organ expanded (stage 6) and ray ventral petals started to elongate (stage 7). However, a significant decrease of *SvDIV1B* transcript levels was detected only in ray florets (stage 8), which coincided with rapid ventral petal elongation (Fig. 4E). In capitulum stage 6-7, *SvDIV1B* in situ hybridization showed that *SvDIV1B* was ubiquitously expressed in florets, including petals of ray florets (Supplemental Fig. S2, A and B). In contrast, very low expression levels were detected by qRT-PCR for *SvRAD* in both ray and disc florets of the six to eight developmental stages analyzed but significantly higher expression levels were observed in all vegetative tissues (Fig. 3C). This is supported by *SvRAD* in situ data, which showed that at late developmental stages, *SvRAD* is almost nondetectable in florets but highly expressed in the vegetative tissues (Supplemental Fig. S2, C and D).

Down-Regulation of a *CYC2* Homolog, *RAY3*, Led to Shorter Ray Florets

To determine the role of ray floret specific *RAY3* expression, we generated *S. vulgaris* transgenic plants with *RAY3* down-regulation. We obtained five independent transgenic lines (Supplemental Fig. S1A), all of which were confirmed to have decreased *RAY3* expression by qRT-PCR (Fig. 5A). In these transgenic lines, mature capitula consistently had significantly shorter ray floret ventral petals while no difference was observed in disc florets, compared to nontransformed controls (Fig. 4, A, G, and S).

To further investigate the morphological changes in petal length at earlier stages, transgenic and wild-type control plants were analyzed by scanning electron microscopy (SEM). In wild-type *S. vulgaris*, ray florets initially consist of five similarly sized petals (two dorsal and three ventral; Fig. 4C, stage 4). As the capitulum develops (Fig. 4E, stage 8), the three fused ventral petals elongate rapidly to form a tongue-shaped ray floret (Fig. 4A, Ra). SEM images showed that the shorter ventral petal phenotype of *RAY3* antisense plants (Fig. 4, A and G) was not evident in stage 4 (Fig. 4, C and I), suggesting that *RAY3* is involved in ventral petal elongation during later developmental stages.

In order to determine whether changes in cell shape or cell number caused the final shorter ray petal phenotype of *RAY3* transgenic plants, we measured width and length of adaxial epidermal cells in ray ventral petals (Fig. 4, F and L). Results showed that ray ventral petal cell width increased in *RAY3* transgenic lines but not cell length, compared to wild-type controls (Fig. 4, U and V). This suggests that down-regulation of *RAY3* caused fewer cells along the proximal-distal axis of the ray ventral petal, indicating that decreased cell division caused shorter ray florets.

SvDIV1B Down-Regulation Led to Longer Ray Petals

qRT-PCR expression data suggested that *SvDIV1B* might play a role in ray and disc floret development. To further determine the role of *SvDIV1B* in floret development, we generated transgenic plants that down-regulated *SvDIV1B* in *S. vulgaris*. We obtained six independent transgenic lines (Supplemental Fig. S1B) and decreased expression levels were confirmed in four independent transgenic lines by qRT-PCR (Fig. 6A). In mature capitula of these *SvDIV1B* transgenic

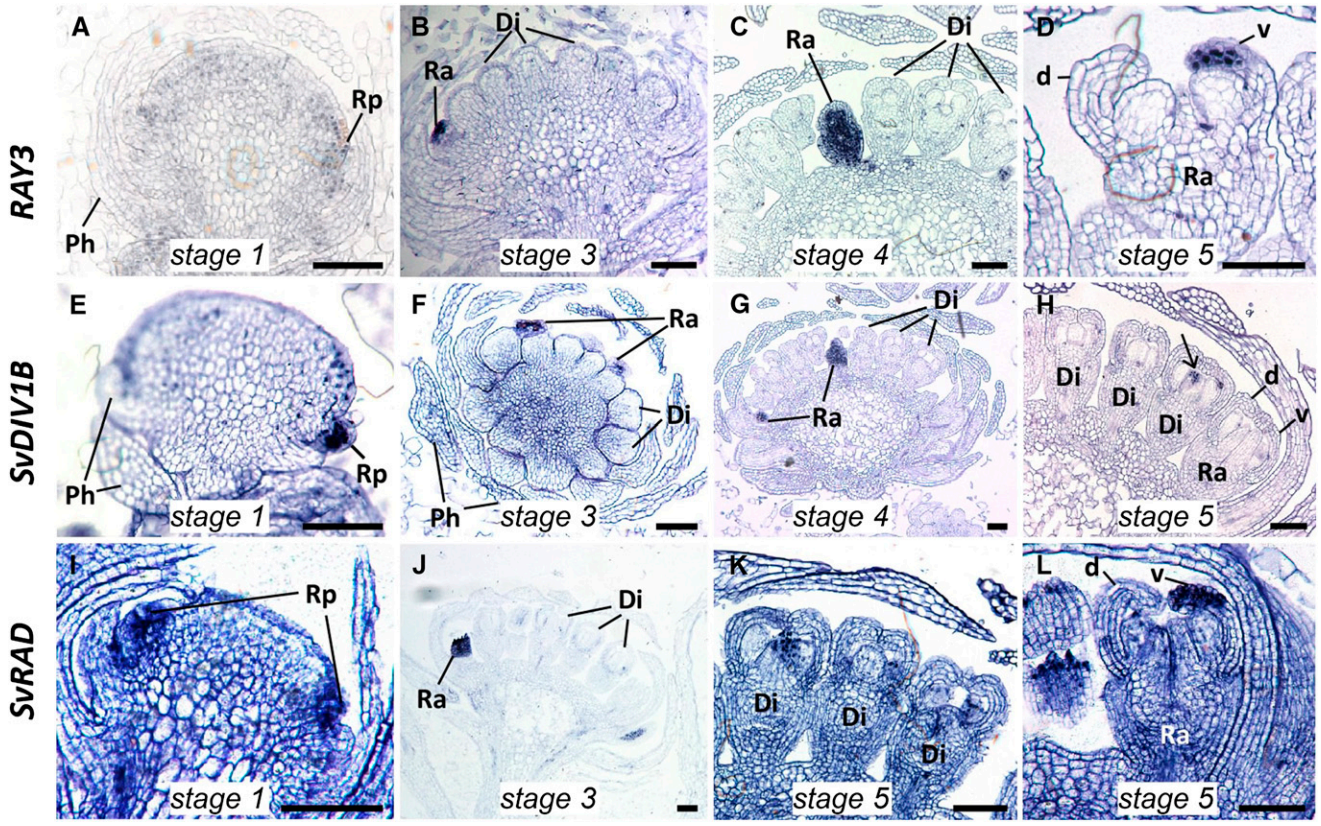

Figure 2. *RAY3*, *SvDIV1B*, and *SvRAD* RNA in situ expression profiles during *S. vulgaris* capitulum development. *RAY3* (A–D), *SvDIV1B* (E–H), and *SvRAD* (I–L) transcripts were restricted to ray primordia (Rp) in stage 1 (A, E, and I) and developing ray florets (Ra) in stage 3 (B, F, and J), stage 4 (C and G) and stage 5 (D, H, K, and L) capitula. Unlike *SvDIV1B* (G and H), transcripts of *RAY3* and *SvRAD* accumulated in the developing ventral (v) petals of ray florets (D and L) but were absent in the disc florets (C and K). Di, Disc florets; Ra, ray florets; Rp, ray primodium; Ph, phyllaries; d, dorsal petal; v, ventral petal. Bars = 100 μm.

plants, ray ventral petals were significantly longer than in wild-type controls, while no effect was observed in disc florets (Fig. 4, A, M, and T).

To study how this long petal phenotype developed in earlier stages, SEM images were taken of *SvDIV1B* transgenic capitula. Longer ventral petals were seen as early as stage 4 (Fig. 4, N and O, stage 4), suggesting that the initiation of ray ventral petals in *SvDIV1B* transgenic plants occurs earlier than in the wild type. After stage 4, longer ray ventral petals were maintained through all the later stages of capitulum development (Fig. 4, M, P, and Q). However, disc floret morphology was not affected by *SvDIV1B* down-regulation at any of the stages studied.

As in the *RAY3* transgenic analysis, we measured individual cell width and length of ray ventral petal epidermal cells of *SvDIV1B* transgenic and wild-type plants (Fig. 4, F and R). Results showed that cell width was not significantly different (Fig. 4U); however, cell length was reduced in transgenic lines compared to wild-type controls (Fig. 4V). Both longer final petal length and shorter individual cell length suggests that the number of cells along the proximal-distal petal axis increased, which implies that reduction of *SvDIV1B* RNA levels led to increased cell division.

Interaction among Floral Symmetry Regulators

In *S. vulgaris*, down-regulation of *RAY3* and *SvDIV1B* had an opposite effect on ray petal length, suggesting their antagonistic roles during ray floret development. To investigate their genetic relationships and interactions with other known floral symmetry regulators, we have analyzed *SvDIV1B*, *RAY1*, *RAY2*, *RAY3*, and *SvRAD* expression levels by qRT-PCR in both *RAY3* and *SvDIV1B* transgenic plants. Results showed that down-regulation of *RAY3* led to reduction of *SvDIV1B* levels in one transgenic line (Fig. 5B) and up-regulation of *SvRAD* in three out of five transgenic lines (Fig. 5C). Furthermore, *RAY1* and *RAY2* transcription levels were significantly reduced in most lines in response to *RAY3* down-regulation (Fig. 5, D and E).

In contrast, down-regulation of *SvDIV1B* expression levels led to up-regulation of both *RAY3* and *SvRAD* in all lines (Fig. 6, B and C) and to down-regulation of *RAY2* in half of the transgenic lines (Fig. 6E). However, *RAY1*

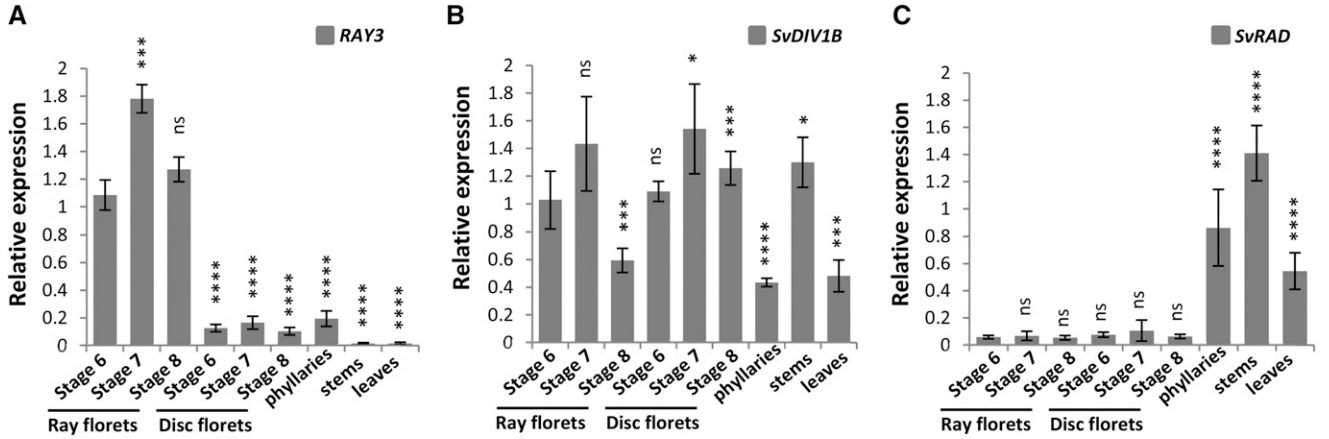

Figure 3. qRT-PCR analysis of *RAY3*, *SvDIV1B*, and *SvRAD* transcripts in developing wild-type *S. vulgaris* capitulum tissues. A, *RAY3* transcription levels were significantly higher in ray floret developmental stages than all the other plant tissues. B, *SvDIV1B* transcription levels were higher in stage 6 and 7, compared to stage 8 ray florets, while disc florets showed similar expression levels in all developmental stages. *SvDIV1B* transcripts were also detected in vegetative tissues. C, *SvRAD* expression levels were very low in all ray and disc floret stages but high in vegetative tissues. Gene expression levels were normalized to *5.8s* rRNA. Asterisks indicate significance using two tailed Student's *t* test when compared to stage 6 ray florets: $*P \leq 0.05$, $***P \leq 0.001$, $****P \leq 0.0001$, and $^{ns}P > 0.05$ (ns, not significant). Error bars are ± SD values of three biological and four technical replicates.

transcription levels were variable in all the *SvDIV1B* transgenic lines (Fig. 6D). Together, our gene expression data suggest that *RAY3* appears to promote *RAY1* and *RAY2*, while *SvDIV1B* inhibits *RAY3* and *SvRAD* and activates *RAY2* (directly or indirectly) during capitulum development.

DISCUSSION

Expression of *RAY3*, *SvDIV1B*, and *SvRAD* Is Restricted to Ray Florets within the Young Capitulum

Here, our phylogenetic analyses showed that *RAY3* was clustered within the *CYC2* subfamily of *TCP* genes known to control flower asymmetry (Fig. 1H). In particular, the *RAY3* gene fragment was shown to be a homolog of the sunflower *HaCYC2b* gene and gerbera *GhCYC4* and *GhCYC9*. While *RAY3* expression was consistent with *GhCYC4* and *GhCYC9* (Tähtiharju et al., 2012), its expression differed from that of *HaCYC2b* (Tähtiharju et al., 2012; Chapman et al., 2008). Our in situ hybridization and qRT-PCR data showed that *RAY3* was expressed mainly in ray florets throughout all stages (Figs. 2 and 3A). The *RAY3* sunflower homolog *HaCYC2b* was initially expressed in ray florets as seen here in *Senecio*; however, later, *HaCYC2b* was expressed across multiple floral and vegetative tissues including disc florets (Tähtiharju et al., 2012; Chapman et al., 2008). Instead, *RAY3* expression was more similar to the sunflower paralogs, *HaCYC2c* and *HaCYC2d*, which were expressed mainly in ray florets throughout all stages. Moreover, two *S. vulgaris CYC* genes, *RAY1* and *RAY2*, were also shown to be specifically expressed in ray floret primordia (Kim et al., 2008). Therefore, although capitulum patterning relies on *CYC2* clade ray floret specific expression, it appears that different Asteraceae lineages have independently recruited distinct *CYC* paralogs for ray floret differentiation (Chapman et al., 2012; Hileman, 2014). Perhaps this is not surprising since ray florets are considered to have evolved multiple times in this family (Panero and Funk, 2008; Hileman, 2014).

Notably, in the early stages of capitulum development, *RAY3* was ubiquitously expressed across the ray floret, which contrasts with the dorsal-specific expression patterns of their homologs in other species with zygomorphic solitary flowers (Corley et al., 2005; Luo et al., 1996; Hileman et al., 2003). The uniform *RAY3* expression in the early ray floret primordium suggests that *RAY3* may be involved in the initiation of all five petals. In the Malpighiaceae-Elatinaceae families, basal species have actinomorphic flowers with uniform *CYC2* expression, whereas derived species have zygomorphic flowers with dorsal-specific *CYC2* expression (Zhang et al., 2010). Therefore, this early uniform *RAY3* expression in the ray floret may resemble the ancestral expression pattern of *CYC2* homologs in these families. However, the fact that their expression was uniform in the young ray floret cannot explain how *CYC* genes establish bilateral symmetry in the ray floret. Unlike *RAY1* and *RAY2*, which are expressed in both dorsal and ventral petals (Supplemental Fig. S2, E–H), in the later stages of capitulum development (stage 5), *RAY3* was exclusively expressed in ray ventral petals (Fig. 2D), which led to their elongation and, therefore, floral zygomorphy in the ray floret. This is in agreement with studies in *G. hybrida*, which show ventral expression of *GhCYC2* in ray florets (Broholm et al., 2008; Juntheikki-Palovaara et al., 2014). In the zygomorphic *Antirrhinum* flower, however, *CYC* is expressed in the dorsal petals (Luo et al., 1996). Although these *CYC* genes have

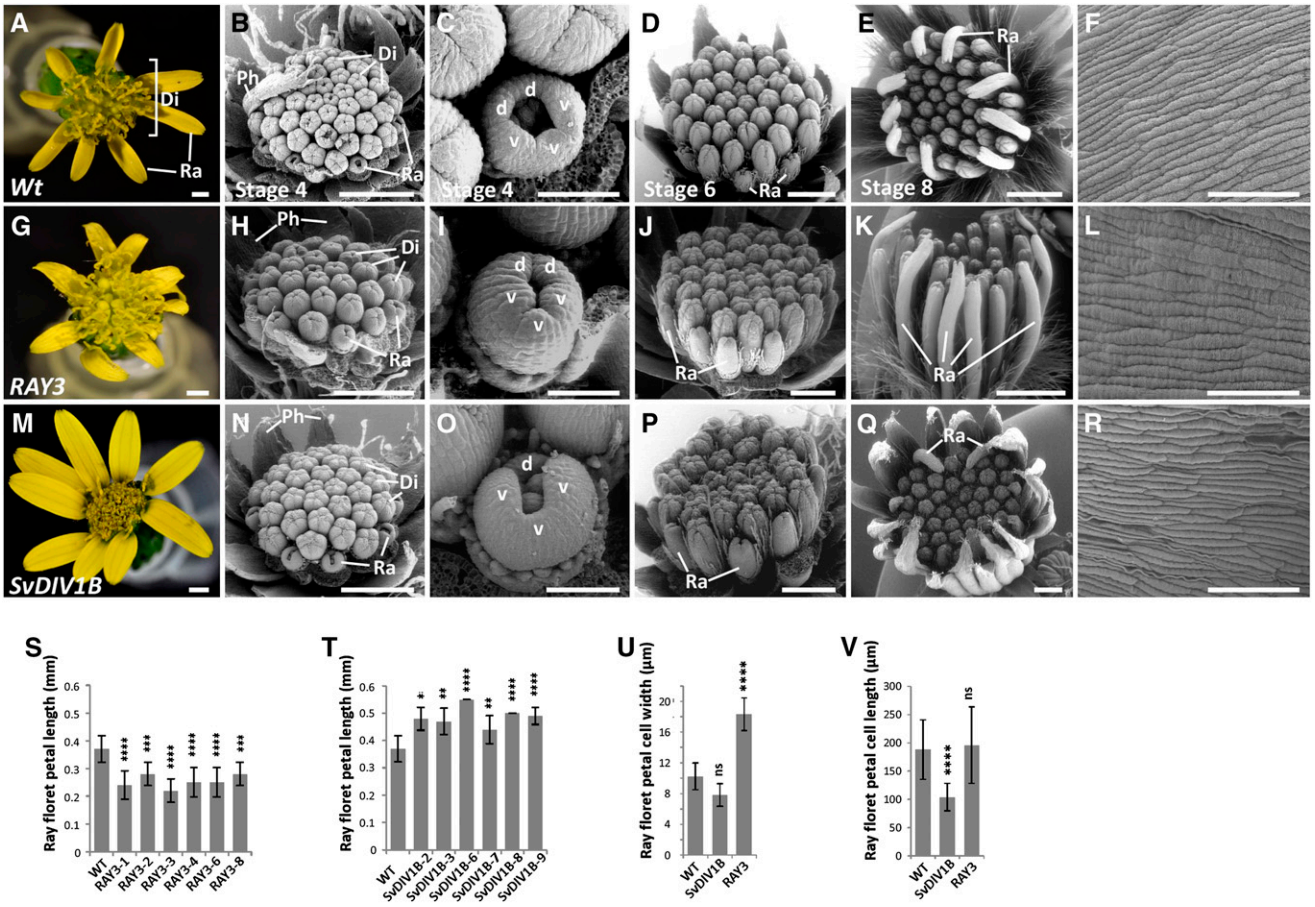

Figure 4. Flower phenotypes of wild-type, *RAY3*, and *SvDIV1B* transgenic plants. A to F, Wild-type (nontransformed) control. G to R, *RAY3* (G–L) and *SvDIV1B* (M–R) down-regulation capitulum and ray floret phenotypes. Di, Disc florets; Ra, ray florets; Ph, phyllaries; d, dorsal petal; v, ventral petal. Bars = 100 μm (C, F, I, L, O, and R), 500 μm (B, D, H, J, N, and P), and 1 mm (A, E, G, K, M, and Q). S to V, Quantitative ray floret phenotypic analysis of wild-type control, *SvDIV1B*, and *RAY3* down-regulation plants. S and T, Ray floret length of wild-type control and several *RAY3* and *SvDIV1B* transgenic lines, respectively. Down-regulation of *RAY3* and *SvDIV1B* had antagonistic effects on ray floret petal length. Down-regulation of *SvDIV1B* significantly increased ray petal length, while *RAY3* down-regulation decreased petal length in all transgenic lines. U and V, Average mature cell width and length of ray floret petal epidermal cells in wild-type control and in several *SvDIV1B* and *RAY3* transgenic lines. U, Cell width was significantly increased in *RAY3* down-regulated lines, while it was not changed in SvDIV1B transgenic lines. V, Down-regulation of *SvDIV1B* expression levels led to a significant ray floret petal cell length reduction, while *RAY3* down-regulation had no effect. Error bars indicate SD values for $n = 10$ plants (S and T) and $n = 20$ plants (U and V) relative to wild-type controls. Asterisks indicate significance in two tailed Student's t test when compared to the wild type: $^{**}P \leq 0.01$, $^{***}P \leq 0.001$, $^{****}P \leq 0.0001$, and $^{ns}P > 0.05$ (ns, not significant).

evolved to express differently in dorsal (*CYC* in *A. majus*) versus ventral (*RAY3* in *S. vulgaris* and *GhCYC2* in *G. hybrida*) domains, it is likely that both genes have maintained similar functions in promoting petal elongation. The fact that loss of *RAY3* expression only partly affected ray petal elongation and did not lead to fully actinomorphic flowers indicates that additional factors such as *RAY2* (Kim et al., 2008) may contribute to the ray petal elongation.

As with *RAY3*, we have found that *SvRAD* expression during early capitulum development (stage 1-4) was restricted to ray florets and absent from disc florets (Fig. 2, I and J). After initial uniform *SvRAD* expression in the ray florets, expression is later restricted to the ventral petals (Fig. 2L), suggesting a role in controlling zygomorphy. This contrasts with dorsal *RAD* expression in *A. majus* but matches the expression pattern of *RAY3*. Our qPCR data showing the low *SvRAD* expression during the later capitulum stages suggests that *SvRAD* may only have an active role in the initial establishment of zygomorphy but not in the elongation of petals. Moreover, this is supported by the fact that variable *SvRAD* expression in *RAY3* transgenics (Fig. 5C) did not correspond to the expected petal phenotypes based on *RAD* function in *A. majus*. To verify this, further functional analyses are required. It is also possible that other *Senecio RAD* genes (yet to be identified) are involved in later petal elongation. Notably, our

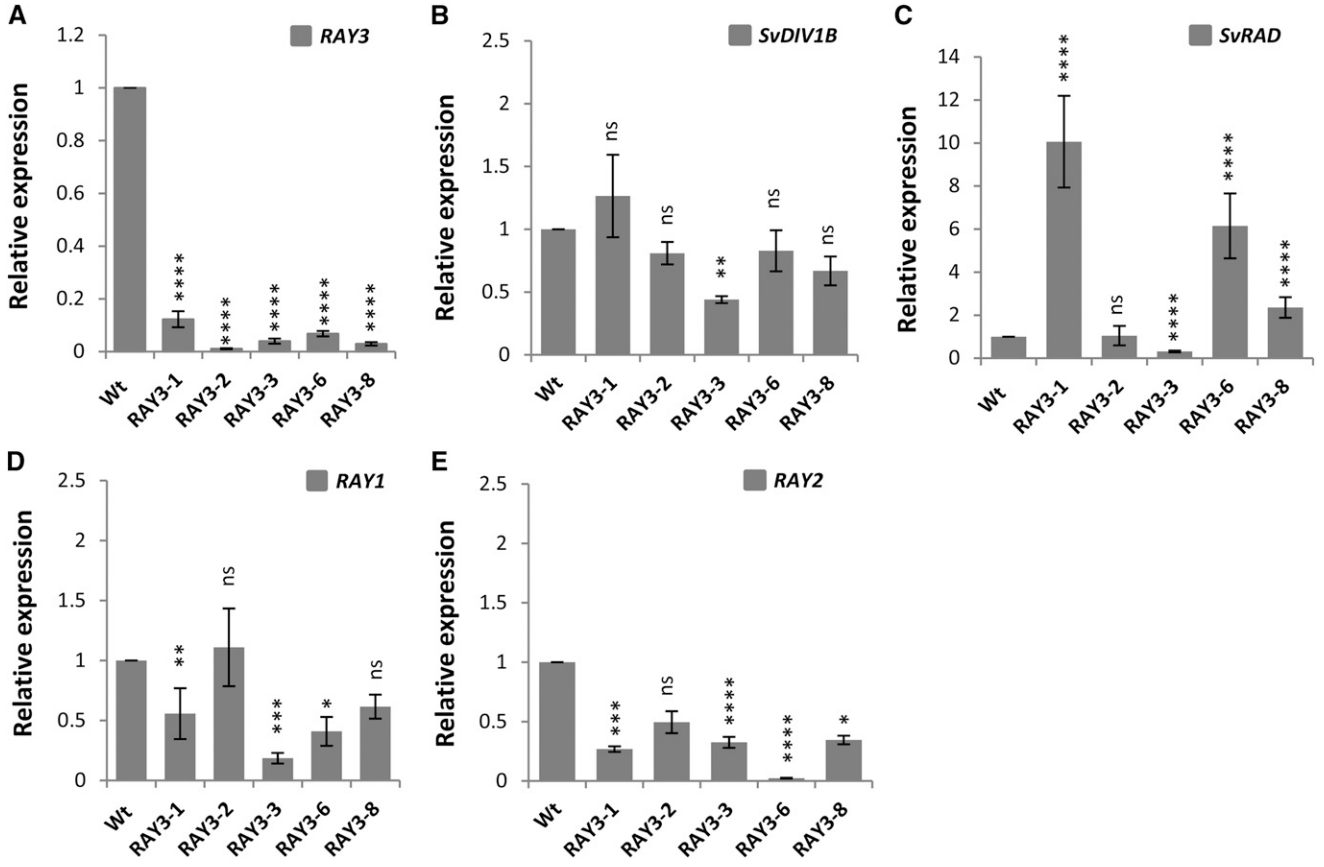

Figure 5. qRT-PCR analysis of flower symmetry gene regulators in *S. vulgaris* wild-type and *RAY3* transgenic capitula (stage 6-8). A, *RAY3* transcription levels were significantly down-regulated in all transgenic lines. B, *SvDIV1B* transcription levels were only reduced in one *RAY3* down-regulated transgenic line. C, *SvRAD* expression levels were significantly increased in three out of five transgenic lines in response to *RAY3* down-regulation. D, *RAY1* transcription levels were significantly reduced in most lines in response to *RAY3* down-regulation. E, *RAY2* transcription expression levels were significantly reduced in most lines in response to *RAY3* down-regulation. Gene expression levels were normalized with *5.8S rRNA* and are shown relative to the wild-type control expression levels. Asterisks indicate significance using two tailed Student's *t* test when compared to the wild type: $*P \leq 0.05$, $**P \leq 0.01$, $***P \leq 0.001$, $****P \leq 0.0001$, and $^{ns}P > 0.05$ (ns, not significant). Error bars are ± SD values of four technical replicates on biological triplicates.

phylogenetic analysis showed that *SvRAD* is not an *AmRAD* ortholog, either suggesting that an *AmRAD* paralog was independently recruited in *Senecio* or that multiple paralogs control floral symmetry in this species.

The initial *SvDIV1B* expression pattern on the other hand is conserved with the *A. majus DIV* ortholog. In *A. majus*, *DIV* expresses throughout the floral meristem and is excluded from dorsal petals at later stages of flower development, which corresponds with dorsal petal elongation (Almeida et al., 1997). In *S. vulgaris*, after the expression of *SvDIV1B* in ray and disc florets, phyllaries, and vegetative tissues (Fig. 3B), a drastic decrease of *SvDIV1B* transcripts was detected in stage 8 ray florets (Fig. 3B), which coincided with the rapid ventral petal elongation (Fig. 4E). Together, these data suggest that *SvDIV1B* needs to be down-regulated in order to achieve ray petal elongation and thus bilateral symmetry. This reduction in *SvDIV1B* expression across the whole ray floret differs from the ventral localization seen in *A. majus*. Together, these *SvDIV1B* and *SvRAD* data provide the first explanation for how *RAD* and *DIV* genes in Asteraceae contribute to bilateral symmetry establishment in the developing ray floret.

RAY3 and *SvDIV1B* Play Antagonistic Roles during Ray Petal Development

Consistent with the role suggested by our *RAY3* and *SvDIV1B* expression data, transgenic plants down-regulating *RAY3* and *SvDIV1B* showed altered petal elongation in ray florets but not in disc florets. In mature capitula, down-regulation of *RAY3* and *SvDIV1B* RNA levels led to significantly shorter or longer ray ventral petals, respectively, while no effect was observed in disc florets (Fig. 4). These changes in ray petal length in both *RAY3* and *SvDIV1B* transgenic plants were caused by alterations in cell division. Ray ventral petal

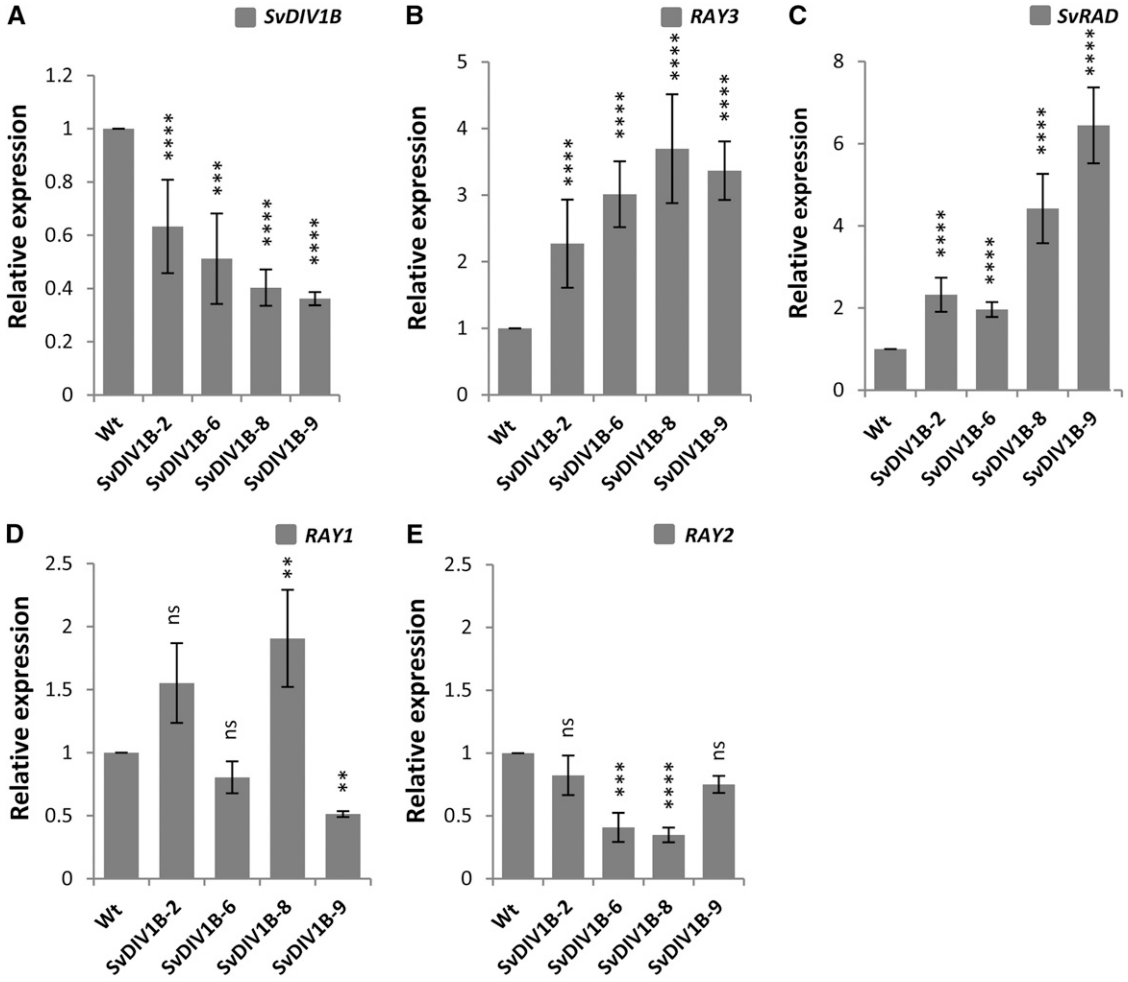

Figure 6. qRT-PCR analysis of flower symmetry gene regulators in *S. vulgaris* wild-type and *SvDIV1B* transgenic capitula (stage 6-8). A, *SvDIV1B* transcription levels were significantly down-regulated in all transgenic lines. B and C, *RAY3* (B) and *SvRAD* (C) transcription levels were significantly increased in all *SvDIV1B* down-regulated transgenic lines. D, *RAY1* transcription levels were variable for all the *SvDIV1B* down-regulated transgenic lines. E, *RAY2* transcription expression levels were significantly reduced in half of the *SvDIV1B* down-regulated transgenic lines. Gene expression levels were normalized with 5.8S rRNA and are shown relative to the expression levels of wild-type control. Asterisks indicate significance using two tailed Student's *t* test when compared to the wild type: $^{**}P \leq 0.01$, $^{***}P \leq 0.001$, $^{****}P \leq 0.0001$, and $^{ns}P > 0.05$ (ns, not significant). Error bars are ± SD values of three biological and four technical replicates.

cell width increased (Fig. 4U) in *RAY3* transgenic lines but not cell length (Fig. 4V). Contrarily, in *SvDIV1B*, cell width of ray ventral petals was similar (Fig. 4U), while cell length was reduced (Fig. 4V) in transgenic plants. Therefore, these results indicate that down-regulation of *RAY3* causes a decrease in cell division leading to shorter ray florets, whereas reducing *SvDIV1B* RNA levels increases cell division, which in turn leads to longer ray floret phenotypes. Taken together, these results suggest that both genes have antagonist effects on ray petal length via cell division and that *RAY3* is likely to promote while *SvDIV1B* is likely to repress cell division during wild-type ray petal development. These results are consistent with several other studies, which connect TCP genes to cell proliferation in various plant developmental processes (Efroni et al., 2008; Nath et al., 2003; Palatnik et al., 2003; Koyama et al., 2007; Hervé et al., 2009; Costa et al., 2005).

These results also suggest that the recruitment of *RAY3* and *SvDIV1B* activity to ray florets is likely to be a critical evolutionary step to differentiate bilateral ray florets from radial disc florets. However, the fact that down-regulation of *RAY3* alone could not convert ray florets into disc florets suggests that several *CYC* genes, e.g. *RAY1* and *RAY2*, were recruited for ray floret identity and zygomorphy. Given that *SvDIV1B* transgenic phenotypes were confined to ray ventral petals but *SvDIV1B* RNA expression was uniform in the ray floret, other dorsoventral genetic components should interact with *SvDIV1B* for bilateral symmetry to be established in these florets. *SvRAD* could be a gene candidate to determine the dorsoventral symmetry of ray florets by

interacting with *SvDIV1B* as in other species (Raimundo et al., 2013). However, to confirm this hypothesis, the function of *SvRAD* needs to be further investigated.

Regulatory Relationships of Floral Symmetry Genes Are Altered to Promote Ray Florets in *S. vulgaris*

We have found that novel gene regulatory interactions among floral symmetry genes exist in *S. vulgaris*. Our results showed that during capitulum development, down-regulation of *RAY3* led to reduction of *RAY1* and *RAY2* RNA levels (Fig. 5, D and E). As the DNA sequence identity in the cloned *RAY3* region and corresponding *RAY1* and *RAY2* fragments are 66% and 59%, respectively, cross-suppression based on sequence identity is unlikely. For this reason, the qRT-PCR data are likely to reflect a positive regulatory relationship between *CYC* paralogs. In *A. majus*, the *backpetals*

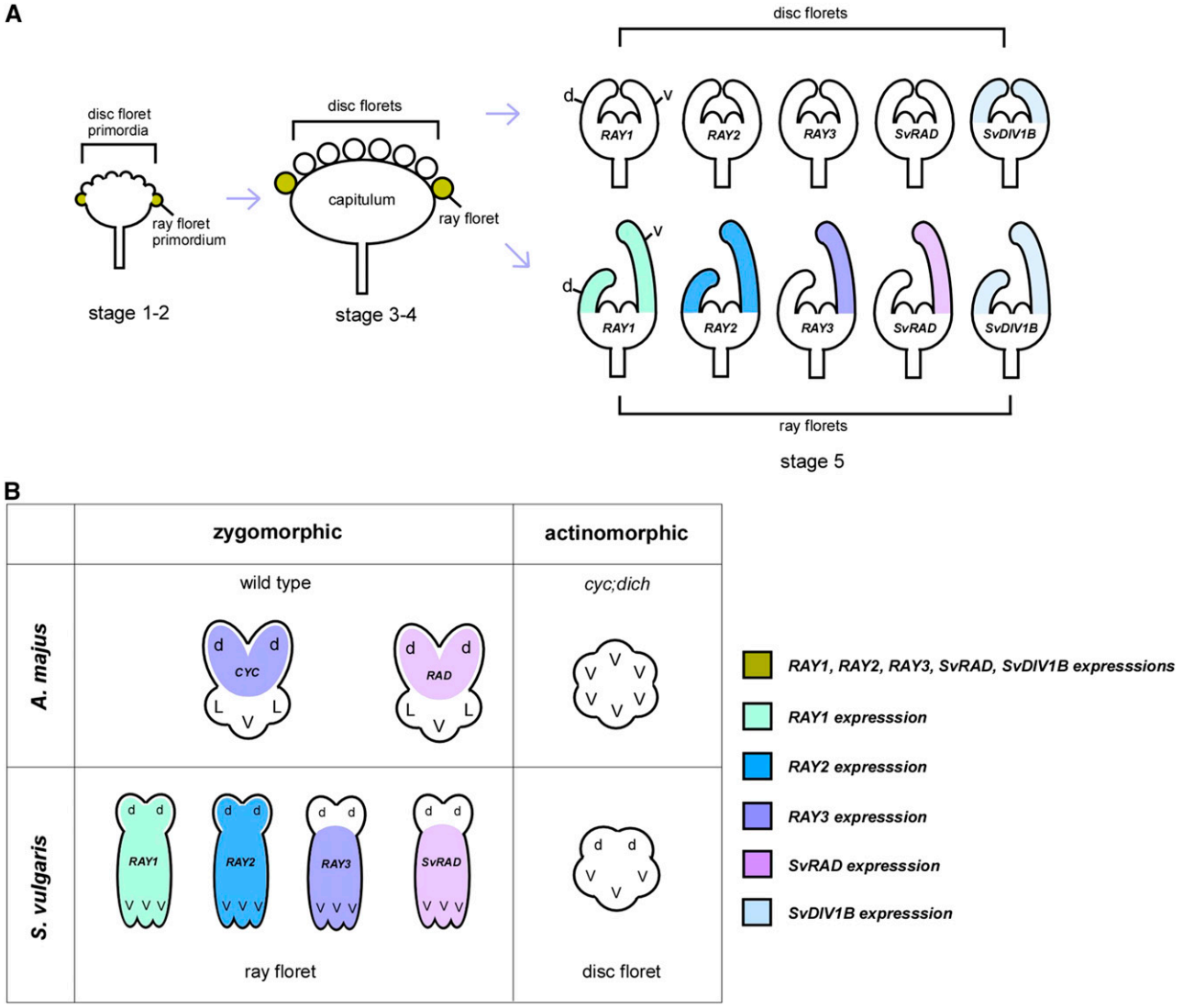

Figure 7. A schematic model showing flower symmetry gene expression during capitulum and floret development in *S. vulgaris*. A, Initially, *RAY* (*CYC-like*) genes, *SvRAD* and *SvDIV1B* are expressed in the emerging ray floret primordia to give the competency to develop bilateral symmetry in these florets, which sets them apart from radial disc florets. Later, as petals emerge in a ray floret, *RAY3* and *SvRAD* are expressed in the ventral petals to set up the dorsoventral symmetry by promoting the ventral petal elongation. During ray ventral petal elongation, *RAY1* and *RAY2* are also present in the ventral domain and involved in petal growth (Kim et al., 2008). *SvDIV1B* appears to play a role in counterbalancing the *RAY* gene activities although its role in dorsal ray petal and disc floret development remains to be investigated. B, The expression patterns of *CYC* genes are diversified in *S. vulgaris*. To generate two different florets, *RAY* genes are exclusively recruited only to the zygomorphic ray florets. However, a subset of *RAY* genes such as *RAY3* acquired ventral petal specific expression and promotes ventral petal growth. This is comparable to the *CYC* activity in the dorsal petal domain where it promotes dorsal petal growth to establish zygomorphy in *A. majus*. No *RAY* gene expression in actinomorphic disc florets is analogous to actinomorphic *cyc;dich* flowers. d, Dorsal petal; L, lateral petal; V, ventral petal.

mutant, caused by ectopic expression of *CYC*, did not alter the other *CYC2* gene, *DICH* expression in the dorsal petals (Luo et al., 1999). Furthermore, *CYC* activity was shown to be unaltered in *dich* mutants, indicating that the regulation of these *CYC* genes is independent during dorsal petal development (Luo et al., 1999). However, in *Primulina heterotricha*, *CYC1C* regulates *CYC2D* and vice versa, showing the presence of regulatory relationships between *CYC* genes as seen here (Yang et al., 2012).

In addition, in *A. majus*, *CYC* activates *RAD*, which is a key interaction in determining floral dorsal and lateral identity (Corley et al., 2005). However, our results showed that in *RAY3* down-regulation transgenic lines, *SvDIV1B* and *SvRAD* expression levels were variable, suggesting that in *S. vulgaris* capitula *RAY3* does not interact (directly) with these genes to regulate ray floret dorsoventral identity. One possibility is that in *S. vulgaris*, the *CYC-RAD* interaction may involve *CYC* paralogs other than *RAY3* alone.

While *RAY3* promoted *RAY2* expression during ray floret development, *SvDIV1B* repressed *RAY3* and *SvRAD* but activated *RAY2*. Floral bilateral symmetry in *A. majus* involves the action of *CYC* and *DICH* that activate *RAD*, which in turn down-regulates *DIV* activity in dorsal petals (Raimundo et al., 2013; Corley et al., 2005; Costa et al., 2005; Almeida et al., 1997). However, there has been no evidence as to whether *DIV* can feedback to regulate these genes during flower development. To the best of our knowledge, this is the first report that shows a regulatory role of *SvDIV1B* on dorsal identity genes (*RAY2*, *RAY3*, and *SvRAD*), suggesting that a more complex gene network may exist in capitulum development. Interestingly, in *SvDIV1B* antisense transgenic lines, up-regulation of *RAY3* (by *DIV1B* down-regulation) did not lead to *RAY2* up-regulation; *RAY2* was instead down-regulated. This suggests that regulation of *RAY2* by *RAY3* involves a more complex network and may rely on the presence/activity of other genetic components such as *SvDIV1B*. However, further studies are required to identify such interactions in *Senecio*.

Inference for Ray Floret Dorsoventral Symmetry

Based on our expression and functional analyses of *RAY3* and *SvDIV1B*, we propose the following model (Fig. 7) to explain the establishment of floral symmetry in a capitulum. During early capitulum development (Fig. 7A, stage 1-4), key players of floret symmetry, *RAY1*, *RAY2*, *RAY3*, *SvRAD*, and *SvDIV1B* are expressed in the ray florets to give the competency to develop bilateral symmetry in these florets, which sets them apart from radial disc florets. As petals emerge (stage 5), *RAY3* accumulates in the ventral ray petals, which leads to rapid ventral petal elongation, thus to the bilateral symmetry in the ray floret (Fig. 7A). Given that *RAY3* promotes and *SvDIV1B* represses petal growth, persistent *RAY3* expression (accompanied by decreasing *SvDIV1B* levels) may explain rapid ventral petal elongation in the ray florets at the later stages (stage 8). This also highlights that in *S. vulgaris*, the roles of *CYC* (*RAY3*) and *DIV* (*SvDIV1B*) in petal elongation are conserved. However, to create ray floret bilateral symmetry via ventral petal outgrowth, similar to *GhCYC2* in gerbera (Broholm et al., 2008), the *RAY3* activity was shifted to the ventral region of the ray floret in *S. vulgaris*, contrasting to the *CYC-RAD* activity in the dorsal region in (non-Asteraceae) species with solitary flowers (Luo et al., 1996; Corley et al., 2005; Zhang et al., 2010). In this model (Fig. 7), all *RAY* genes are exclusively recruited to the zygomorphic ray florets but not to actinomorphic disc florets. Moreover, a subset of *RAY* genes, such as *RAY3*, acquired ray ventral petal specific expression, which in turn promotes petal growth in this domain. This highlights how the diversification of *CYC* genes played an important role in creating a complex structure such as the capitulum in the Asteraceae family and how different regulatory interactions between floral symmetry genes have been recruited in angiosperms to control flower shape.

MATERIALS AND METHODS

Plant Material and Growth Conditions

Senecio vulgaris RR genotype plants were grown from seed for *in vitro* tissue culture. Seeds were vapor-gas sterilized (Clough and Bent, 1998) prior to transferring to germination media (half-strength Murashige and Skoog [MS] [w/v] media and 0.8% [w/v] plant agar [Melford] at pH 5.8). In order to increase *S. vulgaris* seed germination rate, filter sterilized 0.1% (w/v) Gibberellic Acid A3 (Melford) was added to seeds. Plates were transferred to a Percival tissue culture cabinet (22°C, 16 h light, 100 μmol m^{-2} s^{-1}) for 2 weeks. Seedlings were transferred to magenta boxes containing full-strength (w/v) MS medium (3% Suc [w/v] and 0.8% [w/v] plant agar [Melford] at pH 5.8). After 1 month, plants were ready to be used for tissue culture transformation. Plants for seed harvesting and phenotypic analysis were grown in pots with Sinclair compost in a growth chamber under 16-h-light photoperiod (150 μmol m^{-2} s^{-1}) at 24°C until flowering stage. Images of flower phenotypes were recorded with a dissecting scope (Leica S8AP0) using a Nikon D3100 camera. Several stages of *S. vulgaris* capitula were used for in situ hybridizations (stage 1-5), qRT-PCR (stage 6-8), and SEM (stages 4, 6, and 8). For wild-type qRT-PCR tissue specificity analyses, ray and disc florets were dissected separately under a dissecting microscope (Leica S8AP0), and phyllaries, developing leaves (1-cm-long leaves), and stems were also harvested. For *RAY3* and *SvDIV1B* down-regulation transgenic qRT-PCR analyses, inflorescences consisting of capitula (stages 6–8) were harvested. We defined *S. vulgaris* capitulum stages 1 to 8 of development as follows: stage 1, capitula with emerging ray floret primordia; stage 2, capitula with emerging disc floret primordia; stage 3, capitula with ray and disc florets already formed but without floret lateral organs such as sepals and petals; stage 4, capitula with lateral organ primordia emerging within both florets; stage 5, lateral organs expanding within both florets; stage 6, ventral petal start to elongate within the ray florets; stage 7, ray and disc reach similar florets length; stage 8, further elongation of ventral petals within the ray florets.

Gene Isolation and Vector Constructs

A *CYC* homolog genomic DNA (gDNA) fragment (*RAY3*) of 297 bp was cloned from *S. vulgaris* RR genotype (DNA from the inflorescence consisting of stage 1-8 capitula) using degenerative primers (DeCYC-1/DeCYC-2; Supplemental Table S1). These primers were designed based on several *Senecio* and sunflower (*Helianthus annuus*) *CYC2* sequences from two plants species obtained from the GenBank database (FJ356699.1, FJ356698.1, FJ356702.1, FJ356701.1, EU088371, and EU088372), and the following gradient PCR conditions were used for amplification: 98°C for 3 min, 98°C 15 s, temperature of 45 to 51°C for 30 s, and 72°C for 1 min, repeated for 36 cycles and followed by an

extension of 5 min at 72°C. Partial sequences for *SvCYC4*, *SvCYC5*, *SvCYC6*, and *SvCYC7* genes were obtained by RACE-PCR from total RNAs of *Senecio* R/R young inflorescence (Edinburgh accession), with degenerate primers designed according to a conserved region of TCP genes: G775 and G873 (Supplemental Table S1). A 824-bp *DIV* homolog was also cloned from *S. vulgaris* RR genotype (DNA from the inflorescence consisting of stage 1-8 capitula) using previously reported degenerative primers (Howarth and Donoghue, 2009). The DeDIVForw-1/DeDIVRev-1 pair (Supplemental Table S1) was used to amplify *DIV1B* fragment using the above PCR conditions with a few modifications (temperature of 41 to 48°C). Moreover, we isolated a 299-bp *RAD* homolog fragment from *S. vulgaris* cDNA of capitulum inflorescences. We also used this template to clone a 179-bp *RAD* gene fragment using degenerative primers (DeRADForw/DeRADRev; Supplemental Table S1). These primers were designed on *RAD*-like and MYB domain gene sequences from five plant species: NM_001050197.1 (*Oryza sativa*), NM_106181.1 (*Arabidopsis thaliana*), NM_120086.2 (Arabidopsis), NM_001246920.1 (*Solanum lycopersicum*), NM_001249151.1 (*Glycine max*), and AY954971.1 (*Antirrhinum majus*). PCR conditions were the same as described above with a few modifications (temperature of 42°C). Amplified PCR products were cloned into the pGEM-T easy vector (Promega) for sequencing. To make the antisense constructs, specific primers were then designed for both *SvDIV1B* and *RAY3* gene fragments using restriction enzyme sites for directional cloning into the binary vector pBI121 (Clontech). All PCR reactions were performed using Phusion DNA Polymerase (Thermo Fisher Scientific), 2.5 mM dNTPs (Bioline), and 10 μM primers (Eurofins). See primer sequences in Supplemental Table S1.

Phylogenetic Analysis

ML phylogenetic trees for *RAY3*, *SvDIV1B*, and *SvRAD* were obtained using amino acid and DNA sequences. Protein alignments were performed with the ClustalX2 program (Thompson et al., 2002), and ML trees were generated using the RAXML website (http://phylobench.vital-it.ch/raxml-bb/index.php; Stamatakis et al., 2008) with 500 bootstrap replications. For the CYC proteins, 99 amino acids were used, which included the conserved TCP and R domains. For DIV proteins, we generated the ML tree using 95 amino acids, which included the conserved SANT domains. The ML RAD tree was generated using 83-bp DNA sequences, which also included the conserved SANT domain. The species abbreviations are shown in as follows: *Aragoa abietina* (*Aa*), *Aragoa cundinamarcensis* (*Ac*), *Antirrhinum majus* (*Am*), *Arabidopsis thaliana* (*At*), *Bournea leiophylla* (*Bl*), *Cryptothladia chinensis* (*Cc*), *Centranthus macrosiphon* (*Cm*), *Diervilla sessilifolia* (*Ds*), *Digitalis purpurea* (*Dp*), *Dipelta floribunda* (*Df*), *Epimedium sagittatum* (*Es*), *Fedia cornucopiae* (*Fc*), *Fragaria vesca* (*Fv*), *Gerbera hybrida* (*Gh*), *Glycine max* (*Gm*), *Gratiola officinalis* (*Go*), *Helianthus annuus* (*Ha*), *Heptacodium miconioides* (*Hm*), *Kolkwitzia amabilis* (*Ka*), *Lonicera x bella* (*Lb*), *Lonicera morrowii* (*Lm*), *Lonicera reticulata* (*Lr*), *Leycesteria* sp. (*Lsp*), *Medicago truncatula* (*Mt*), *Mohavea confertiflora* (*Mc*), *Plantago major* (*Pm*), *Polypremum procumbens* (*Pp*), *Populus trichocarpa* (*Pt*), *Rhytidophyllum auriculatum* (*Ra*), *Ricinus communis* (*Rc*), *Sixalix atropurpurea* (*Sa*), *Sambucus cerulea* (*Sc*), *Senecio vulgaris* (*Sv*), *Symphoricarpos orbiculatus* (*So*), *Valerianella eriocarpa* (*Ve*), *Veronica chamaedrys* (*Vc*), *Viburnum davidii* (*Vd*), *Vitis vinifera* (*Vv*), *Weigela hortensis* (*Wh*), and *Wulfenia carinthiaca* (*Wc*).

In Situ Hybridizations

Riboprobe synthesis and in situ hybridizations of *RAY3*, *SvDIV1B*, and *SvRAD* genes were performed using the protocol described previously (Garcês and Sinha, 2009b). In situ hybridization for *RAY1* and *RAY2* were performed as previously described (Kim et al., 2008). To clone the *SvDIV1B* 191-bp exon from 824-bp gDNA fragment in the pGEM easy-T (Promega), we used the specific primer set SvDIV1BF/SvDIV1BR (see Supplemental Table S1 for primer sequences). To synthesize the in situ hybridization RNA probes, the 270-bp *RAY3*, 179-bp *SvRAD*, and 191-bp *SvDIV1B* gene fragments, which were cloned in the pGEM easy-T vector, were PCR amplified using the universal M13 forward and reverse primers present in the plasmid backbone and treated as described previously (Garcês and Sinha, 2009b). All fragments were amplified using Phusion DNA polymerase (Thermo Fisher Scientific) and the following PCR conditions: 98°C for 3 min, 98°C 15 s, temperature of 55°C for 30 s, and 72°C for 1 min, repeated for 36 cycles and followed by an extension of 5 min at 72°C. One microgram of PCR product was used to transcribe both sense (−) and antisense (+) single-stranded RNA probes using T7 and SP6 promoters, digoxigenin-UTP, and the T7 and SP6 RNA polymerases contained in DIG labeling kit (Roche Applied Science). In situ hybridizations were performed according to the previous protocol (Garcês and Sinha, 2009b) with the following modifications: Inflorescences of *S. vulgaris* capitula (1 to 5 capitula stages) were fixed in paraformaldehyde (Alfa Aesar) solution (4% paraformaldehyde [v/v], 100 mM PBS, and 1% DMSO) for 16 h at 4°C, embedded in Surgipath Paraplast Plus paraffin (Leica Biosystems), and sectioned into 9-μm sections. Sections were deparaffinized with Histo-clear II (Agar Scientific) and rehydrated via an ethanol series. Slides were then treated for 25 min at 37°C with 0.065 mg/mL proteinase K (Sigma-Aldrich). Probe hybridization was carried out overnight at 50°C. After hybridization, slides were treated as described previously (Garcês and Sinha, 2009b). Signal detection was performed using antidigoxigenin conjugated to alkaline phosphatase fab fragments (Roche) as the secondary antibody. The alkaline phosphatase substrate 5-bromo-4-chloro-3-indolyl-phosphate/nitro blue tetrazolium (BCIP/NBT; Promega), was prepared according to the manufacturer's specifications prior to application to the sections. Tissues were incubated for 3 to 6 h on average with BCIP/NBT or until a purple/blue color developed (gene expression). Samples were viewed using a Leica DMR microscope, and electronic images were acquired using SPOT advanced software (SPOT Imaging Solutions). Image color balancing and cropping was performed using Adobe Photoshop CS6, and figures were executed using Canvas X software (ADC Systems).

qRT-PCR Expression Analysis

For qRT-PCR analysis of wild-type *S. vulgaris* tissue-specific gene expression, ray and disc florets were dissected and harvested from capitula at several developmental stages (stage 6-8), as well as phyllaries, developing leaves (1-cm-long leaves), and stems (Fig. 3). For gene regulatory relationship studies, inflorescences of capitula (stage 6-8) were used for qRT-PCR analyses (Figs. 5 and 6). All tissues were immediately frozen after harvesting into liquid nitrogen and saved at −80°C until further analyses. Total RNA was extracted using RNeasy Mini Kit (Qiagen). Five micrograms of total RNA was DNase I treated according to the manufacture's specifications (Promega) and used for cDNA synthesis using the Untergasser protocol (Untergasser et al., 2007). qRT-PCR primers were designed using Primer3 software (Untergasser et al., 2007), and qRT-PCR was performed on a ABI Prism 7000 PCR machine (Applied Biosystems). Reactions were performed using SensiFAST SYBR Hi-ROX Kit (Bioline) according to manufacturer's specifications with primers at a final concentration of 500 nM and RNA at 10 ng per reaction. Annealing temperatures were kept to ±1°C of 60°C with target GC content of 50 to 60%. The PCR efficiency of each target gene was calculated using LinReg (Hårdstedt et al., 2005), and the gene expression levels were determined using the comparative threshold cycle method (Schmittgen and Livak, 2008). All qRT-PCR was performed on biological triplicates in technical quadruplicates, as described previously (Etchells et al., 2012). Statistical analysis and graphs were performed in Excel (Microsoft). Samples were normalized to *5.8s* rRNA and *18s* rRNA control genes. Both control genes gave similar expression levels for all the genes tested. We chose *5.8s* rRNA control gene for gene analysis, and ± SD error bars were calculated on three biological and four technical replicates per sample.

Plant Transformation

For the plant transformation, *RAY3* and *DIV1B*, 270- and 824-bp gDNA fragments, respectively, were cloned in antisense orientation into pBI121 carrying the 35S promoter and the *neomycin phosphotransferase II* (*NPTII*) gene, which confers kanamycin resistance to positive transformants. One-month-old *S. vulgaris* RR genotype plants grown in sterile conditions in magenta boxes were used for the transformation experiments. Leaves were harvest and sectioned in 1-cm^2 explants for transformation. *Agrobacterium tumefaciens* (GV3101) carrying the antisense constructs was inoculated into liquid LB medium containing 100 mg/L kanamycin (Melford) and 50 mg/L Rifampicin (Melford) and shaken overnight at 30°C. Cells were collected by centrifugation and resuspended to an OD_{600} of 0.5 to 0.8 nm in liquid full-strength (w/v) MS medium with no antibiotics (MS0) for plant infection. Acetosyringone (100 μM; Sigma-Aldrich) was added to this suspension to enhance DNA transfer. The bacterial suspension was shaken in the dark and at room temperature until needed. *S. vulgaris* leaf explants were cocultivated with the *A. tumefaciens* suspension for 20 min, blotted dry, and transferred to petri dishes containing coculture (without selection) callus/shoot inducing media (full-strength MS salts, 3% Suc [w/v], 1 mg/L thidiazuron [Sigma-Aldrich], 0.1 mg/L 1-naphthaleneacetic acid [Sigma-Aldrich] at pH 5.8, and 7.5g/L Phytoagar [Sigma-Aldrich]). Plates were transferred to a Percival tissue culture cabinet at 22°C for 3 d in the dark. Explants were then transferred to calli/shoot inducing media containing

40 mg/L kanamycin (Melford) and 250 mg/L cefotaxime (Melford) antibiotics to select for positive transformants (MS1). These plates were incubated in the Percival tissue culture cabinet at 22°C with a photoperiod of 16 h light (100 μmol m^{-2} s^{-1}). Explants were subcultured to fresh MS1 medium every 2 weeks until the appearance of calli with shoots. Once shoots were formed, they were removed from calli and transferred to magenta boxes containing root induction media (MS2) (half-strength MS salts, 3% [w/v] Suc, pH 5.8, and 7.5g/L Phytoagar) with antibiotics (100 mg/L kanamycin and 250 mg/L cefotaxime). Rooted shoots were transferred to new fresh MS2 media in Magentas every month or earlier if needed. Once transgenic plants had a well-developed root system, plants were transferred to soil. Plant trays were covered with a humidity lid, and this lid was slowly removed over the period of a week to adjust plants to their new environment. Transgenic plants were ready to be analyzed 2 months later. In this species, the whole process to obtain transgenic plants ready to be analyzed can take a total of 6 to 8 months. The presence of *RAY3* and *SvDIV1B* antisense transgenes was confirmed by PCR using gDNA extracted from five and six independent transgenic lines with 35S Forw and RAY3-5′*Sac*I reverse primer or SvDIV1B-5′*Sac*I, respectively (Supplemental Table S1).

SEM Analysis

Several flower head developmental stages (very young, 1–2 mm; medium, 2–3 mm; and mature, 3–4 mm flowers) from wild-type nontransformed plants and from several *SvDIV1B* and *RAY3* down-regulation transgenic lines were fixed for SEM and viewed as described previously (Garcês and Sinha, 2009a). Dehydrated samples were taken through critical point drying using a Polaron critical point dryer (Quorum Technologies) and were mounted onto SEM stubs (Agar Scientific) using carbon tape (Agar Scientific). Samples were then sputter coated with carbon for 90 s using a Polaron E5100 sputter coater (Quorum Technologies). SEM images were obtained directly from a FEI Quanta 250 FEG electron microscope (FEI) at 5 to 10 kV accelerating voltage. Image color balancing and cropping were performed using Adobe Photoshop CS6, and figures were executed using Canvas X software (ADC Systems).

Capitulum Phenotypic Analysis

SEM images were used to measure mature ray floret petal adaxial epidermis cell length and width in wild-type controls, *RAY3* and *SvDIV1B* down-regulation transgenic lines. Statistical analysis and graphs were performed in Excel. The SD values were calculated on $n = 10$ plants for ray floret length an on $n = 20$ plants for ray floret width relative to wild-type controls. Stars indicate significance in two-sample tailed Student's t test assuming unequal variances with $^{**}P \leq 0.01$, $^{***}P \leq 0.001$, $^{****}P \leq 0.0001$, and $^{ns}P > 0.05$ (ns, not significant).

Accession Numbers

Gene sequence information can be found on the NCBI website under the following accession numbers: KT722935 (*RAY3*), KT722933 (*SvDIV1B*), KT722936 (*SvRAD*), *SvCYC4* (KU663021), *SvCYC5* (KU663022), *SvCYC6* (KU663023), *SvCYC7* (KU663024), and *DIV3B* (KU666938).

Supplemental Data

The following supplemental materials are available.

Supplemental Figure S1. PCR amplification of *RAY3* and *SvDIV1B* transgenes.

Supplemental Figure S2. In situ hybridization showing the expression pattern of *SvDIV1B*, *SvRAD*, *RAY1*, and *RAY2* in *S. vulgaris*.

Supplemental Table S1. Primer sequences used for cloning genes, making constructs, and expression analysis.

ACKNOWLEDGMENTS

We thank Dr. Tobias Starborg in the Electron Microscopy Facility of the Faculty of Life Sciences for his assistance and the Wellcome Trust for equipment grant support to the Electron Microscopy Facility.

Received March 8, 2016; accepted May 10, 2016; published May 12, 2016.

LITERATURE CITED

Almeida J, Galego L (2005) Flower symmetry and shape in *Antirrhinum*. Int J Dev Biol **49:** 527–537

Almeida J, Rocheta M, Galego L (1997) Genetic control of flower shape in *Antirrhinum majus*. Development **124:** 1387–1392

Boyden GS, Donoghue MJ, Howarth DG (2012) Duplications and expression of radialis-like genes in Dipsacales. Int J Plant Sci **173:** 971–983

Broholm SK, Tähtiharju S, Laitinen RAE, Albert VA, Teeri TH, Elomaa P (2008) A *TCP* domain transcription factor controls flower type specification along the radial axis of the Gerbera (Asteraceae) inflorescence. Proc Natl Acad Sci USA **105:** 9117–9122

Busch A, Zachgo S (2007) Control of corolla monosymmetry in the Brassicaceae *Iberis amara*. Proc Natl Acad Sci USA **104:** 16714–16719

Chapman MA, Leebens-Mack JH, Burke JM (2008) Positive selection and expression divergence following gene duplication in the sunflower *CYCLOIDEA* gene family. Mol Biol Evol **25:** 1260–1273

Chapman MA, Tang S, Draeger D, Nambeesan S, Shaffer H, Barb JG, Knapp SJ, Burke JM (2012) Genetic analysis of floral symmetry in Van Gogh's sunflowers reveals independent recruitment of *CYCLOIDEA* genes in the Asteraceae. PLoS Genet **8:** e1002628

Citerne H, Jabbour F, Nadot S, Damerval C 2010. The evolution of floral symmetry. *In* J. C. Kader, M. Delseny, eds, Advances in Botanical Research, Vol 54, pp. 85–137, Elsevier

Citerne HL, Pennington RT, Cronk QCB (2006) An apparent reversal in floral symmetry in the legume *Cadia* is a homeotic transformation. Proc Natl Acad Sci USA **103:** 12017–12020

Clough SJ, Bent AF (1998) Floral dip: a simplified method for Agrobacterium-mediated transformation of *Arabidopsis thaliana*. Plant J **16:** 735–743

Corley SB, Carpenter R, Copsey L, Coen E (2005) Floral asymmetry involves an interplay between TCP and MYB transcription factors in Antirrhinum. Proc Natl Acad Sci USA **102:** 5068–5073

Costa MMR, Fox S, Hanna AI, Baxter C, Coen E (2005) Evolution of regulatory interactions controlling floral asymmetry. Development **132:** 5093–5101

Crepet WL (1996) Timing in the evolution of derived floral characters: Upper Cretaceous (Turonian) taxa with tricolpate and tricolpate-derived pollen. Rev Palaeobot Palynol **90:** 339–359

Cubas P, Lauter N, Doebley J, Coen E (1999) The *TCP* domain: a motif found in proteins regulating plant growth and development. Plant J **18:** 215–222

Efroni I, Blum E, Goldshmidt A, Eshed Y (2008) A protracted and dynamic maturation schedule underlies Arabidopsis leaf development. Plant Cell **20:** 2293–2306

Endress PK (1999) Symmetry in flowers: Diversity and evolution. Int J Plant Sci (Suppl) **160:** S3–S23

Etchells JP, Provost CM, Turner SR (2012) Plant vascular cell division is maintained by an interaction between PXY and ethylene signalling. PLoS Genet **8:** e1002997

Feng X, Zhao Z, Tian Z, Xu S, Luo Y, Cai Z, Wang Y, Yang J, Wang Z, Weng L, et al (2006) Control of petal shape and floral zygomorphy in *Lotus japonicus*. Proc Natl Acad Sci USA **103:** 4970–4975

Garcês H, Sinha N (2009a) Fixing and sectioning tissue from the plant *Kalanchoë daigremontiana*. Cold Spring Harb Protoc **2009:** t5301

Garcês H, Sinha N (2009b) *In situ* hybridization in the plant *Kalanchoë daigremontiana*. Cold Spring Harb Protoc **2009:** t5302

Hårdstedt M, Finnegan CP, Kirchhof N, Hyland KA, Wijkstrom M, Murtaugh MP, Hering BJ (2005) Post-transplant upregulation of chemokine messenger RNA in non-human primate recipients of intraportal pig islet xenografts. Xenotransplantation **12:** 293–302

Hervé C, Dabos P, Bardet C, Jauneau A, Auriac MC, Ramboer A, Lacout F, Tremousaygue D (2009) *In vivo* interference with *AtTCP20* function induces severe plant growth alterations and deregulates the expression of many genes important for development. Plant Physiol **149:** 1462–1477

Hileman LC (2014) Bilateral flower symmetry–how, when and why? Curr Opin Plant Biol **17:** 146–152

Hileman LC, Kramer EM, Baum DA (2003) Differential regulation of symmetry genes and the evolution of floral morphologies. Proc Natl Acad Sci USA **100:** 12814–12819

Howarth DG, Donoghue MJ (2006) Phylogenetic analysis of the "ECE" (CYC/TB1) clade reveals duplications predating the core eudicots. Proc Natl Acad Sci USA **103:** 9101–9106

Howarth DG, Donoghue MJ (2009) Duplications and expression of *DIVARICATA-like* genes in dipsacales. Mol Biol Evol **26:** 1245–1258

Howarth DG, Martins T, Chimney E, Donoghue MJ (2011) Diversification of *CYCLOIDEA* expression in the evolution of bilateral flower symmetry in Caprifoliaceae and Lonicera (Dipsacales). Ann Bot (Lond) **107:** 1521–1532

Juntheikki-Palovaara I, Tähtiharju S, Lan T, Broholm SK, Rijpkema AS, Ruonala R, Kale L, Albert VA, Teeri TH, Elomaa P (2014) Functional diversification of duplicated CYC2 clade genes in regulation of inflorescence development in *Gerbera hybrida* (Asteraceae). Plant J **79:** 783–796

Kim M, Cui M-L, Cubas P, Gillies A, Lee K, Chapman MA, Abbott RJ, Coen E (2008) Regulatory genes control a key morphological and ecological trait transferred between species. Science **322:** 1116–1119

Koyama T, Furutani M, Tasaka M, Ohme-Takagi M (2007) TCP transcription factors control the morphology of shoot lateral organs via negative regulation of the expression of boundary-specific genes in Arabidopsis. Plant Cell **19:** 473–484

Luo D, Carpenter R, Copsey L, Vincent C, Clark J, Coen E (1999) Control of organ asymmetry in flowers of Antirrhinum. Cell **99:** 367–376

Luo D, Carpenter R, Vincent C, Copsey L, Coen E (1996) Origin of floral asymmetry in Antirrhinum. Nature **383:** 794–799

Nath U, Crawford BCW, Carpenter R, Coen E (2003) Genetic control of surface curvature. Science **299:** 1404–1407

Palatnik JF, Allen E, Wu X, Schommer C, Schwab R, Carrington JC, Weigel D (2003) Control of leaf morphogenesis by microRNAs. Nature **425:** 257–263

Panero JL, Funk VA (2008) The value of sampling anomalous taxa in phylogenetic studies: major clades of the Asteraceae revealed. Mol Phylogenet Evol **47:** 757–782

Preston JC, Hileman LC (2009) Developmental genetics of floral symmetry evolution. Trends Plant Sci **14:** 147–154

Raimundo J, Sobral R, Bailey P, Azevedo H, Galego L, Almeida J, Coen E, Costa MMR (2013) A subcellular tug of war involving three MYB-like proteins underlies a molecular antagonism in Antirrhinum flower asymmetry. Plant J **75:** 527–538

Reardon W, Gallagher P, Nolan KM, Wright H, Cardeñosa-Rubio MC, Bragalini C, Lee C-S, Fitzpatrick DA, Corcoran K, Wolff K, Nugent JM (2014) Different outcomes for the MYB floral symmetry genes *DIVARICATA* and *RADIALIS* during the evolution of derived actinomorphy in Plantago. New Phytol **202:** 716–725

Schmittgen TD, Livak KJ (2008) Analyzing real-time PCR data by the comparative C(T) method. Nat Protoc **3:** 1101–1108

Stamatakis A, Hoover P, Rougemont J (2008) A rapid bootstrap algorithm for the RAxML Web servers. Syst Biol **57:** 758–771

Tähtiharju S, Rijpkema AS, Vetterli A, Albert VA, Teeri TH, Elomaa P (2012) Evolution and diversification of the CYC/TB1 gene family in Asteraceae–a comparative study in Gerbera (Mutisieae) and sunflower (Heliantheae). Mol Biol Evol **29:** 1155–1166

Thompson JD, Gibson TJ, Higgins DG 2002. Multiple sequence alignment using ClustalW and ClustalX. *In* A.D. Baxevanis, ed, Current Protocols in Bioinformatics, 00:2.3:2.3.1–2.3.22

Trow AH (1912) On the inheritance of certain characters in the common groundsel, *Senecio vulgaris* L., and its segregates. J Genet **2:** 239–276

Untergasser A, Nijveen H, Rao X, Bisseling T, Geurts R, Leunissen JAM (2007) Primer3Plus, an enhanced web interface to Primer3. Nucleic Acids Res **35:** W71–W74

Wang Z, Luo Y, Li X, Wang L, Xu S, Yang J, Weng L, Sato S, Tabata S, Ambrose M, et al (2008) Genetic control of floral zygomorphy in pea (*Pisum sativum* L.). Proc Natl Acad Sci USA **105:** 10414–10419

Yang X, Pang H-B, Liu B-L, Qiu Z-J, Gao Q, Wei L, Dong Y, Wang Y-Z (2012) Evolution of double positive autoregulatory feedback loops in CYCLOIDEA2 clade genes is associated with the origin of floral zygomorphy. Plant Cell **24:** 1834–1847

Zhang W, Kramer EM, Davis CC (2010) Floral symmetry genes and the origin and maintenance of zygomorphy in a plant-pollinator mutualism. Proc Natl Acad Sci USA **107:** 6388–6393

Zhong J, Kellogg EA (2015a) Duplication and expression of CYC2-like genes in the origin and maintenance of corolla zygomorphy in Lamiales. New Phytol **205:** 852–868

Zhong J, Kellogg EA (2015b) Stepwise evolution of corolla symmetry in CYCLOIDEA2-like and RADIALIS-like gene expression patterns in Lamiales. Am J Bot **102:** 1260–1267

Zhou X-R, Wang Y-Z, Smith JF, Chen R (2008) Altered expression patterns of *TCP* and *MYB* genes relating to the floral developmental transition from initial zygomorphy to actinomorphy in Bournea (Gesneriaceae). New Phytol **178:** 532–543